

## Intruder States and the Onset of Deformation in the Neutron-Deficient Even-Even Polonium Isotopes

N. Bijnens, P. Decrock, S. Franchoo, M. Gaelens, M. Huyse, H.-Y. Hwang,\* I. Reusen, J. Szerypo,<sup>†</sup>  
J. von Schwarzenberg,<sup>‡</sup> and J. Wauters

*Instituut voor Kern- en Stralingsfysika, KULeuven, Celestijnenlaan 200 D, B-3001 Leuven, Belgium*

J. G. Correia, A. Jokinen, P. Van Duppen, and The ISOLDE Collaboration

*CERN, CH-1211 Geneva 23, Switzerland*

(Received 28 April 1995)

Alpha- and beta-decay studies of mass-separated Rn and At nuclei reveal the existence of a low-lying  $0^+$  state in  $^{196,198,200,202}\text{Po}$ . The excited  $0^+$  states are interpreted as proton-pair excitations across the  $Z = 82$  shell gap leading to a deformed state, coexisting with the spherical ground state. It is shown that with decreasing neutron number the deformed configuration intrudes to lower excitation energy, increasingly mixing into the ground state.

PACS numbers: 23.60.+e, 21.60.Cs, 23.20.Nx, 27.80.+w

Different shapes, coexisting at low energies, form a well-established phenomenon in nuclei near closed shells [1,2]. In particular at (Pb) and just below (Hg and Pt) the  $Z = 82$  proton-shell closure, extensive studies on odd- and even-mass nuclei, using different experimental approaches such as radioactive decay, in-beam, and laser spectroscopy, have made it possible to develop nuclear models describing the transition from sphericity to deformation or vice versa [1,2]. These models assume that the deformation-driving mechanism is based on the interaction of neutrons (open shell) with proton particle-hole excitations through the  $Z = 82$  shell. A stringent test of these theoretical descriptions would be the identification of shape coexistence above the  $Z = 82$  closed shell. The equivalence between particles and holes should lead to low-lying deformed states, also called intruder states, in the Bi isotopes, where they are indeed observed [1,3,4], as well as in the even-even Po and Rn isotopes. Furthermore, the occurrence of intruder states above  $Z = 82$  will make a verification of the intruder spin classification scheme proposed by Heyde *et al.* [5,6] possible. Total potential energy surface calculations for the light Po isotopes using a Nilsson potential with a Strutinsky type of shell correction and pairing [7,8] or a Woods-Saxon potential and monopole pairing [9,10] give at first sight conflicting results: from a very flat potential with only shallow local minima [7,8,10] to a very pronounced oblate minimum at  $\beta \approx -0.17$  well separated from the broader more spherical minimum [9]. However, shallow minima can lead to well-defined states with different deformation [2,10]. May *et al.* [9] predict that the oblate deformed minimum becomes the ground state for the lightest Po isotopes (from  $^{194}\text{Po}$  onwards). A strong fingerprint of shape coexistence in even nuclei is the observation of low-lying  $0^+$  states with rotational-like bands built on top of them [2]. Although eventually the high-spin members of these bands can become yrast, it is difficult to observe the low-lying  $0^+$  bandhead with in-beam

techniques. They can, however, be fed in  $\beta$  or  $\alpha$  decay and an extensive systematics has been collected below and at the  $Z = 82$  shell closure [2,11–13]. In a previous study we reported the existence of a low-lying  $0^+$  state in  $^{198}\text{Po}$  populated in the  $\alpha$  decay of  $^{202}\text{Rn}$  [11,14]. In this Letter we report three newly identified  $0_2^+$  states in the neutron-deficient Po isotopes together with their feeding and decay properties. We advocate that this information forms a firm experimental basis for the occurrence of shape coexistence in these nuclei.

The neutron-deficient  $^{198,200}\text{Rn}$  isotopes were produced in a spallation reaction of 1.0 GeV protons on a thorium-carbide target at the ISOLDE on-line mass separator at CERN [15]. A cooled transfer line was used between target chamber and ion source in order to suppress non-noble-gas radioactive isotopes like Po and At and to obtain an essentially pure Rn beam. The mass-separated  $^{200}\text{Rn}$  beam was implanted in a tape that moved the implanted activity periodically from the implantation station to a decay station. The cycle time was determined by the half-life of the Rn nucleus. Coincidence setups were used to focus on weak alpha branches leading to excited states. An alpha-plastic detector coincidence setup was mounted at the implantation station and an alpha-photon setup at the decay station. We used PIPS type  $\alpha$  detectors (150 mm<sup>2</sup> active surface), a LEGe (low-energy germanium, 1500 mm<sup>2</sup> active surface) detector to detect x rays and low-energy photons, and a plastic scintillator (4 mm thick, 20 mm diameter) for conversion electron detection. A more detailed description of the detection setup can be found in Ref. [14]. As the proton beam has a pulsed structure with a repetition time of a multiplet of 1.2 s, the time between proton beam impact and detected alpha event was recorded in order to obtain information on the half-life. As the half-life of  $^{198}\text{Rn}$  is too short for tape transport, only an  $\alpha$ -BaF<sub>2</sub> (5 mm thick, 30 mm diameter) coincidence detector setup was used at the implantation

TABLE I. The  $\alpha$  decay properties of  $^{202,200,198}\text{Rn}$ . A list of energies ( $E_\alpha$ ), half-lives ( $T_{1/2}$ ), relative  $\alpha$  intensities ( $I_\alpha$ ), hindrance factors (HF), and involved levels from our work unless stated otherwise. The hindrance factors are calculated using the method of Rasmussen [19].

	$E_\alpha$ (keV)	$T_{1/2}$ (s)	$I_\alpha$ (%)	HF	Level assignment in Po
$^{202}\text{Rn} \rightarrow ^{198}\text{Po}$	6641 <sup>a</sup>	9.85 <sup>a</sup>	100	1	$0^+$ ground state
	5841 <sup>b</sup>		$1.8(6) \times 10^{-3}$ <sup>b</sup>	19(6) <sup>b</sup>	$0^+$ at 816 keV <sup>b</sup>
$^{200}\text{Rn} \rightarrow ^{196}\text{Po}$	6902 <sup>a</sup>	1.06 <sup>c</sup>	100	1	$0^+$ ground state
	6355(6)		$8.1(7) \times 10^{-3}$	85(7)	$0^+$ at 558(7) keV
	6454(14)		$6(2) \times 10^{-3}$	180(60)	$2^+$ at 463 keV <sup>d</sup>
$^{198}\text{Rn} \rightarrow ^{194}\text{Po}$	7205(5)	0.064(2)	100	1	$0^+$ ground state
	6893(8)		$7(2) \times 10^{-2}$	72(20)	$2^+$ at 319 keV <sup>e</sup>

<sup>a</sup>Reference [17]. <sup>b</sup>Reference [11]. <sup>c</sup>Reference [16]. <sup>d</sup>Reference [8]. <sup>e</sup>Reference [18].

station. A selection of the results obtained on mass 202 [14], mass 200, and mass 198, relevant for this Letter is given in Table I.

Figure 1 shows prompt (a) and random (b) projections out of the  $\alpha$ - $e$  coincidence matrix, taken at mass 200. Because of the high count rate in the electron detector, the ground state to ground state alpha transitions of  $^{200}\text{Rn}$  and  $^{196}\text{Po}$  are visible in the prompt and random spectrum. Only two  $\alpha$  lines, at 5769(6) and 6355(6) keV, clearly have a prompt coincident character, limiting the multipolarity of the transitions deexciting the levels fed by these  $\alpha$  lines to  $E0$ ,  $E1$ ,  $M1$ , and  $E2$ . The 5769 keV  $\alpha$  line was previously assigned as the  $\alpha$  decay of  $^{196}\text{Po}$ , the  $\alpha$ -decay daughter of  $^{200}\text{Rn}$ , feeding the  $0^+$  intruder state at 769 keV in  $^{192}\text{Pb}$  [13]. The 6355 keV  $\alpha$  line shows the same half-life behavior as the ground state  $\alpha$  line of  $^{200}\text{Rn}$  [1.06(2) s [16]]. Figure 1(c) shows a part of the LEGe spectrum gated by the 6355 keV line, showing Po  $KX$  rays in coincidence. No coincidences with  $\gamma$  rays were observed. This and the fact that the electrons in coincidence with the 6355 keV  $\alpha$  line have an energy of 480(80) keV, leads us to conclude that the 6355 keV  $\alpha$  line belongs to the decay of  $^{200}\text{Rn}$  and that it feeds a low-lying  $0^+$  state in  $^{196}\text{Po}$  at 558(7) that decays essentially via an  $E0$  transition to the ground state. The intensity of a possible  $E2$  transition of 95(7) keV towards the  $2^+$  state at 463 keV is less than 30%. A third  $\alpha$  line at 6454(14) keV, belonging to the  $\alpha$  decay of  $^{200}\text{Rn}$ , was identified in coincidence with the  $2^+ \rightarrow 0^+$  (463 keV)  $\gamma$  transition in  $^{196}\text{Po}$ .

The last known even isotope of the neutron-deficient Rn isotopes is  $^{198}\text{Rn}$ . We remeasured the  $\alpha$ -decay energy as 7205(5) keV and the half-life as 64(2) ms, which are in agreement with the literature values of 7196(10) keV and 50(9) ms [16]. A second  $\alpha$  line, of 6893(8) keV, can be attributed to the decay of  $^{198}\text{Rn}$ . Out of the energy spectrum of the  $\text{BaF}_2$  detector, gated by the 6893 keV  $\alpha$  line, and its time structure we can conclude that the 6893 keV  $\alpha$  line feeds an excited level in Po at 318(8) keV, which decays by gamma emission to the  $0^+$  ground state. We tentatively assign a  $J^\pi = 2^+$  to this state at 318 keV, which is in agreement with a recent in-beam study of  $^{194}\text{Po}$  at the ATLAS in Argonne [18]. No statistical significant evi-

dence for feeding of a  $0^+$  state is present. This is probably due to a high hindrance factor (HF) that can be expected on the basis of our results on the heavier Rn isotopes. The hindrance factor of the  $\alpha$  line feeding the  $0^+$  state increases from 19 to 85 when going from  $^{202}\text{Rn}$  to  $^{200}\text{Rn}$ . The  $^{200}\text{Rn}$   $\alpha$ -decay hindrance factor is the highest ever observed for  $\Delta L = 0$  decay. Probably this can be understood as a typical phase transition problem where the hindrance factor depends strongly on small differences in the configuration

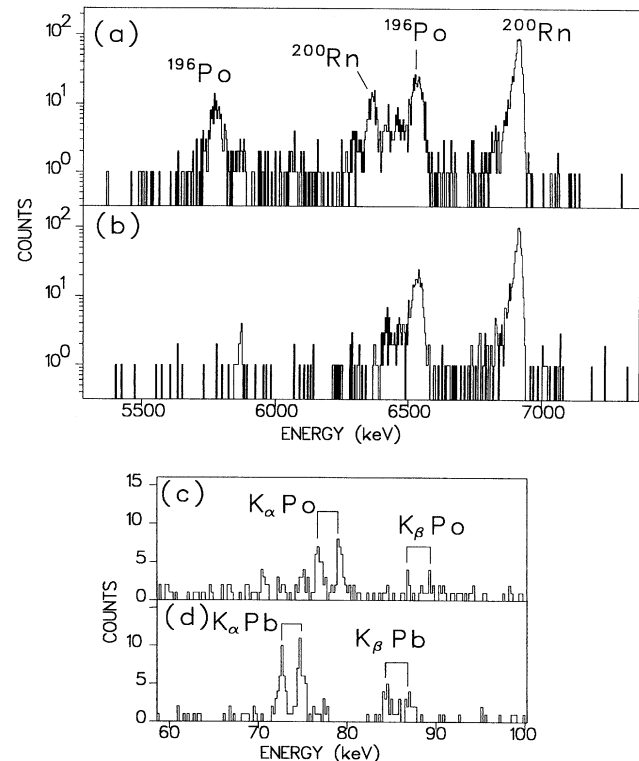


FIG. 1. The  $\alpha$  spectrum, taken at mass 200, coincident with prompt electrons (a) and random electrons (b). Furthermore, the x-ray spectrum gated on the 6355 keV  $\alpha$  line (c) and, as a comparison, the x-ray spectrum gated on the 5769 keV  $\alpha$  line (d).

mixing amplitudes between the intruder and normal states [11,20].

For the  $\beta$ -decay studies, the  $^{200,202}\text{At}$  nuclei were produced in the reaction of 200 MeV  $^{20}\text{Ne}$  on  $^{\text{nat}}\text{Re}$  at the LISOL facility [21] in Louvain-la-Neuve. The mass-separated activity was implanted on an aluminized Mylar tape in order to move it periodically to a decay position. Time-sequential  $\gamma$ - and electron-singles spectra and  $\gamma$ - $\gamma$ - $t$ ,  $\gamma$ - $e$ - $t$ , and  $\gamma$ - $x$ - $t$  coincidences were taken. The detailed report on the  $\beta$ -decay schemes of  $^{200,202}\text{At}$  will be presented in a forthcoming paper [22]. Here we will limit the discussion to transitions with a strong  $E0$  character. Out of the singles and coincidence data it was possible to place these transitions with a pure or enhanced  $E0$  character in the level scheme, identifying an excited  $0_2^+$  state in  $^{202}\text{Po}$  and excited  $0_2^+$ ,  $2_2^+$ , and  $4_2^+$  states in  $^{200}\text{Po}$  (see Table II).

In Fig. 2 we present the low-energy level systematics (positive parity states only) of the even-even neutron-deficient Po isotopes as a function of neutron number between  $N = 110$  and  $N = 126$ . As discussed in Ref. [24], the  $8^+$  and  $6^+$  states have a rather pure  $(\pi h_{9/2})^2$  broken-pair character, while the  $4^+$  and  $2^+$  states show a more complex behavior. The first  $2^+$  state stays at a constant excitation energy from  $^{208}\text{Po}$  down to  $^{200}\text{Po}$  but then decreases steadily. In addition, second excited  $2^+$  and  $4^+$  states with enhanced  $E0$  components in the transitions to the first excited  $2^+$  and  $4^+$  states were observed in  $^{196,198}\text{Po}$  by Alber *et al.* [8] and in  $^{200}\text{Po}$  (this work). Finally, the observation of  $0_2^+$  states whose decay is dominated by a ground state  $E0$  transition, completes the picture of shape coexistence in the light Po isotopes. The characteristic lowering of the excitation energy of the  $0_2^+$ ,  $2_2^+$ , and  $4_2^+$  states when reducing the neutron number towards midshell between  $N = 82$  and 126 is similar as in the Pb, Hg, and Pt isotopes and is a further fingerprint for shape coexistence [1,2].

An interpretation of the energy level systematics as a gradual change from a broken pair configuration to a more vibrational type of excitations is questionable on the basis of the energy position of the  $0_2^+$  state and its decay pattern (mainly to the ground state) and of the strong  $E0$  component present in the  $2_2^+ \rightarrow 2_1^+$  transition. Kantele [30]

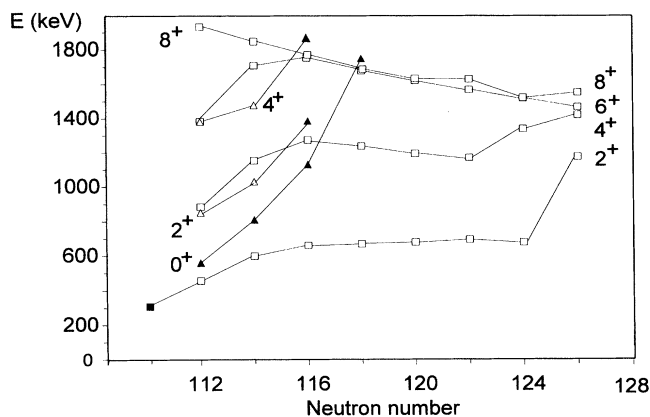


FIG. 2. The low-energy level scheme systematics (positive parity states only) of the neutron-deficient even-even Po isotopes, with the ground state band ( $\square$ ) and the excited deformed band ( $\triangle$ ). Full symbols indicate our work while the open symbols are taken from literature ( $^{198,196}\text{Po}$  [8],  $^{200}\text{Po}$  [24],  $^{202}\text{Po}$  [25],  $^{204}\text{Po}$  [26],  $^{206}\text{Po}$  [27],  $^{208}\text{Po}$  [28],  $^{210}\text{Po}$  [29]).

and Heyde and Meyer [31] pointed out that the latter observation indicates that the two connected states have a different deformation and are mixed. It is this mixing, between the normal states and the intruding deformed band, which causes the deviations in the energy systematics from  $^{198}\text{Po}$  on. A two-level mixing calculation, similar to the one developed for the Pb nuclei [32], gives an increasing contribution of the intruder configuration in the  $2_1^+$  states from 7% in  $^{200}\text{Po}$ , over 31% in  $^{198}\text{Po}$ , and 72% in  $^{196}\text{Po}$  to 88% in  $^{194}\text{Po}$  (for more details see Ref. [22]).

Brenner *et al.* [33] have shown that the excitation energy of the excited  $0^+$  state in the neutron-deficient even-even Pb nuclei follows a down-sloping linear behavior as a function of the so-called  $P$  factor [ $P = N_p N_n / (N_p + N_n)$ ] with  $N_p$  and  $N_n$  the valence nucleon numbers. The  $P$  factor embodies the balance between the deformation-driving quadrupole-quadrupole proton-neutron interaction and the spherical-driving identical nucleon pairing. We have used this formalism to all known  $0^+$  states in the even-even Pt, Hg, Pb, and Po isotopes and plotted the excitation energy versus the  $P$  factor in Fig. 3. Clearly,

TABLE II. Energies  $E$  (keV), conversion coefficients ( $\alpha_K$ ), and some characteristics of pure  $E0$  and highly converted transitions from the  $\beta$ -decay study of  $^{200,202}\text{At}$ . The  $>$  sign in the  $\alpha_{K,\text{expt}}$  coefficients indicates that no  $\gamma$  ray matching the electron energy is observed and pure  $E0$  character is assigned. The theoretical conversion coefficients are based on Ref. [23].

Nucleus	$E$ (keV)	$\alpha_{K,\text{expt}}$	Multipolarity	$\alpha_{K,\text{theor}}$	Coincident with	Assigned to
$^{202}\text{Po}$	1757	$>0.11$	$E0$	$E2 = 0.0022$ $M1 = 0.0047$	Po-KX not with $2^+ \rightarrow 0^+$	$0_2^+(1757) \rightarrow 0_1^+$
$^{200}\text{Po}$	606	0.094(12)	$E0 + M1 + E2$	$E2 = 0.015$ $M1 = 0.066$	Po-KX, $2^+ \rightarrow 0^+$ $4^+ \rightarrow 2^+$	$4_2^+(1883.2) \rightarrow 4_1^+$
	726	0.12(2)	$E0 + M1 + E2$	$E2 = 0.011$ $M1 = 0.041$	Po-KX, $2^+ \rightarrow 0^+$ not with $4^+ \rightarrow 2^+$	$2_2^+(1392.0) \rightarrow 2_1^+$
	1137	$>0.083$	$E0$	$E2 = 0.005$ $M1 = 0.013$	Po-KX not with $4^+ \rightarrow 2^+$ not with $2^+ \rightarrow 0^+$	$0_2^+(1136.5) \rightarrow 0_1^+$

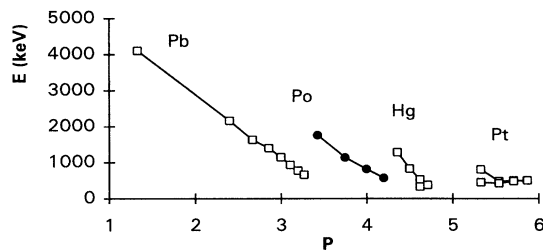


FIG. 3. The excitation energy of all known intruder  $0^+$  states for Pt, Hg, Pb, and Po as a function of the  $P$  factor. The energies are taken from Ref. [2] except for  $^{182}\text{Hg}$  [11] and the Po isotopes.

the Pb, Hg, and Po isotopes [with, respectively,  $\pi(2p-2h)$ ,  $\pi(2p-2h)$ , and  $\pi(4p-2h)$  intruder configurations] exhibit a down-sloping behavior. In contrast the Pt isotopes behave differently, which can be attributed to the high degree of mixing that is believed to take place in  $^{178-186}\text{Pt}$  nuclei [2,11,34]. The decrease in slope with increasing  $P$  for the Po nuclei when approaching midshell, could be an indication of mixing of the deformed intruder state [ $\pi(4p-2h)$ ,  $N_p = 6$ ] with the normal state [ $\pi(2p)$ ]. In fact, as already discussed in previous papers [11,20], the  $\alpha$  decay of  $^{194,196,198}\text{Po}$  reveals that the configuration of these neutron-deficient Po ground states changes from a  $\pi(2p)$  configuration in  $^{198}\text{Po}$  to an admixture of  $\pi(2p)$  and  $\pi(4p-2h)$  in  $^{194}\text{Po}$ . A two-level mixing calculation, using a matrix element of  $\sim 180$  keV, typical for this region [32], gives an increasing contribution of the intruder configuration in the ground state from 1% in  $^{202}\text{Po}$  to 11% in  $^{196}\text{Po}$ . Using a parabolic behavior makes it possible to extrapolate this contribution to 29% in  $^{194}\text{Po}$  and 58% in  $^{192}\text{Po}$ .

In conclusion, we have established an experimental energy systematics of four excited  $0^+$  states in the neutron-deficient even-even Po isotopes,  $^{196-202}\text{Po}$ , strongly resembling the even-even neutron-deficient Pb and Hg isotopes. In addition to the results of Alber *et al.* for  $^{196,198}\text{Po}$ , we identified a  $2^+$  and  $4^+$  candidate for the band built on the excited  $0^+$  state in  $^{200}\text{Po}$ , and finally we observed a candidate for the first excited  $2^+$  state in  $^{194}\text{Po}$ . As is the case below and at the  $Z = 82$  shell closure, also above the shell closure different band structures are present at low energies reflecting the coexistence of different shapes though considerable configuration mixing is observed. The low energy of the first excited state in  $^{194}\text{Po}$  is possible evidence for increased mixing. Experimentally this could be verified in a more detailed fine-structure study in the  $\alpha$  decay of  $^{198}\text{Rn}$  and  $^{192}\text{Po}$ , but due to their short half-lives (ms), such studies should be performed at recoil separators. Another interesting way to study ground state deformation in the light Po isotopes is to measure  $\delta\langle r^2 \rangle$  values with laser spectroscopic methods. The coupling of a neutron to the even-even Po core could eventually lead to odd-even staggering as was observed in the light Hg isotopes [35]. The neutron-deficient Pb

region, with its  $Z = 82$  spherical shell closure and its different proton and neutron superdeformed gaps, exhibits a unique combination of coexisting shapes at low and at high excitation energies and offers an ideal testing ground for nuclear models.

\*Present address: Mokwon University, 24 Mok Dong, Chung-Ku, Taejon, 301-729 Korea.

†Present address: Warsaw University, Institute of Experimental Physics, Hoza 69, 00681 Warsaw, Poland.

‡Present address: University of Notre Dame, Notre Dame, IN 46556.

- [1] K. Heyde *et al.*, Phys. Rep. **102**, 291 (1983); K. Heyde *et al.*, Nucl. Phys. **A466**, 189 (1987).
- [2] J.L. Wood *et al.*, Phys. Rep. **215**, 101 (1992).
- [3] E. Coenen *et al.*, Phys. Rev. Lett. **54**, 1783 (1985).
- [4] M. Huyse *et al.*, Phys. Lett. B **201**, 293 (1988).
- [5] K. Heyde *et al.*, Phys. Rev. C **49**, 559 (1994).
- [6] K. Heyde *et al.*, Phys. Rev. C **46**, 541 (1992).
- [7] C.F. Tsang and S.G. Nilsson, Nucl. Phys. **A140**, 275 (1970).
- [8] D. Alber *et al.*, Z. Phys. A **339**, 225 (1991).
- [9] R. May *et al.*, Phys. Lett. B **68**, 113 (1977).
- [10] W. Satula *et al.*, Nucl. Phys. **A529**, 289 (1991).
- [11] J. Wauters *et al.*, Phys. Rev. Lett. **72**, 1329 (1994).
- [12] P. Van Duppen *et al.*, Phys. Rev. Lett. **52**, 1974 (1984).
- [13] P. Dendooven *et al.*, Phys. Lett. B **226**, 27 (1989).
- [14] J. Wauters *et al.*, Z. Phys. A **344**, 29 (1992).
- [15] E. Kugler *et al.*, Nucl. Instrum. Methods Phys. Res., Sect. B **70**, 41 (1992).
- [16] F. Calaprice *et al.*, Phys. Rev. C **30**, 1671 (1984).
- [17] J. Wauters *et al.*, Phys. Rev. C **47**, 1447 (1993).
- [18] J. Cizewski (private communication).
- [19] J.O. Rasmussen, Phys. Rev. **113**, 1593 (1959).
- [20] D.S. Delion *et al.*, Phys. Rev. Lett. **74**, 3939 (1995).
- [21] M. Huyse *et al.*, Nucl. Instrum. Methods Phys. Res., Sect. B **70**, 50 (1992).
- [22] N. Bijmens *et al.* (to be published).
- [23] F. Rösel *et al.*, At. Data Nucl. Data Tables **21**, 381 (1978).
- [24] A. Maj *et al.*, Nucl. Phys. **A509**, 413 (1990).
- [25] H. Beuscher *et al.*, Phys. Rev. Lett. **36**, 112 (1976).
- [26] R.G. Helmer and C.W. Reich, Phys. Rev. C **27**, 2248 (1983).
- [27] V.B. Brudanin *et al.*, Izv. Akad. Nauk. SSSR, Ser. Fiz. **46**, 45 (1982) [Bull. Acad. Sci. USSR, Phys. Ser. **46**, 34 (1982)].
- [28] B.S. Dzhelepov *et al.*, Izv. Akad. Nauk. SSSR, Ser. Fiz. **47**, 2 (1983) [Bull. Acad. Sci. USSR, Phys. Ser. **47**, 1 (1983)].
- [29] L.J. Jardine *et al.*, Nucl. Phys. **A190**, 261 (1972).
- [30] J. Kantele, in *Heavy Ion and Nuclear Structure*, edited by B. Sikora and Z. Wihelmi (Harwood Academic Publishers, Chur, Switzerland, 1984).
- [31] K. Heyde and R.A. Meyer, Phys. Rev. C **37**, 2170 (1988).
- [32] P. Van Duppen *et al.*, J. Phys. G **16**, 441 (1990).
- [33] D.S. Brenner *et al.*, Phys. Lett. B **293**, 282 (1992).
- [34] G.D. Dracoulis *et al.*, Nucl. Phys. **12**, L97 (1986).
- [35] G. Ulm *et al.*, Z. Phys. A **325**, 247 (1987).